Heavier, Further, Faster: A Simulation-Based Comparative Study of Hybrid VTOL and Multicopter UAVs for Precision Agriculture

Alvaro Lazaro Aguilar
—

***Abstract*—Multirotors have been the dominant type of agricultural spraying drone, yet in other industries winged VTOLs are used for longer missions, because in forward flight their wing carries the weight that a multirotor's rotors carry throughout. This paper asks on which types of farms a hybrid winged VTOL can outperform a multirotor sprayer. The study modelled the multirotor on the DJI Agras T50; the hybrid VTOL is a new quadplane design of our own, built on the T50's hardware, with its winged VTOL components optimised through CFD. Both flew identical spraying jobs over 90 farms of 10 to 150 ha modelled on real farms sourced from four countries, and chosen by size, field spread and fragmentation, each from its best and its worst admissible pad. The missions ran in a GPU-parallel flight simulation in NVIDIA Isaac Lab, driven by CFD force tables. Over all 180 jobs the hybrid sprayed 16.8% more hectares per hour, ground time included, and used 7.8% less energy per hectare. It was faster on 163 jobs, and won on energy once the ferry per sortie exceeded about 1.6 km, as on large, spread or fragmented farms and from poorly placed pads; the multicopter stayed cheaper on small compact farms. The study also found the wing configuration a hybrid VTOL needs to be a viable solution in agricultural spraying, through a change to the wing's existing control surfaces at low speed, flaperons drooped $20°$, that fully restores the lift the wing otherwise loses in the lift rotors' wake and cuts its power by 11% at $10\,\mathrm{m/s}$ with a full tank.**

***Index Terms*—Agricultural UAV, hybrid VTOL, multicopter, aerial spraying, CFD, design optimisation, Isaac Lab.**

I. Introduction

DRONES are increasingly used in precision agriculture to apply crop protection products. Compared with ground sprayers they save chemicals, water and time, leave the crop and soil undamaged [1], and reach wet or obstructed ground that ground rigs cannot [2].

Spraying drones have mostly been multirotors [1], lifted and controlled entirely by their rotors, such as the DJI Agras T50 with eight rotors in coaxial pairs on four arms [3]. Carrying their whole weight on rotors, they pay hover-class power for every metre flown, spraying or not. Operators therefore keep ferries short by moving the launch point with the work [2], with a truck, trailer, generator and tanks that, in one cost model, cost about as much as the drone, and two hours a day for driving between fields [4].

A hybrid winged VTOL hovers on rotors but cruises on a wing. Such sprayers remain rare commercially, on the assumption that spraying, the largest part of a sprayer's flight, is too slow for a wing to pay for its weight, and reviews rate the multirotor the more suitable platform [1]. Still, a sprayer must also fly between pad and crop, and there a winged VTOL cruises at under half its hover power [5], so which aircraft wins depends on how much of the job is ferry, set by the farm's layout and the pad's position. Studies of winged agricultural VTOLs stop at cruise power [6] or spray physics [7]; none compares a hybrid with a multicopter over a whole spraying job.

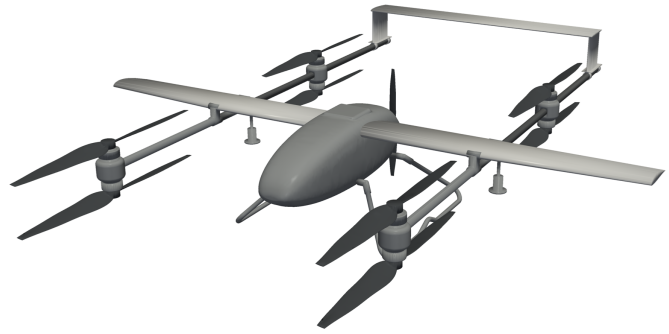

(a)

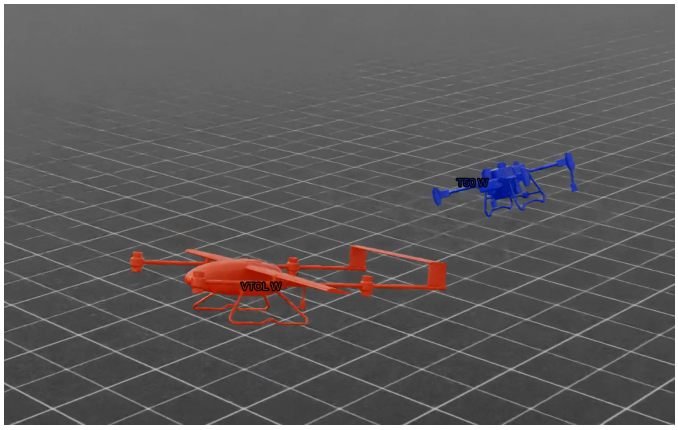

(b)

Fig. 1. (a) The hybrid VTOL sprayer, design D24. (b) Replay of logged missions in Isaac Lab: the multicopter (T50) and the hybrid (VTOL), both from the worst pad (W), flown in separate runs and shown together.

To test that assumption, this paper asks: *in which farm scenarios can a hybrid winged VTOL outperform a multicopter sprayer?* The multicopter is a model of the DJI Agras T50, anchored to its published figures; the hybrid, a lift+cruise design, adds to the T50's parts a wing and tail optimised by CFD and a pusher motor sized to their drag. Both fly identical routes over 90 farms of 10 to $150\,\mathrm{ha}$ modelled on real farms

in four countries, from two pads per farm, in a GPU-parallel simulation built on NVIDIA Isaac Lab [8].

The contributions are:

- a simulation-based operator guide: for farm types by size, field spread, fragmentation and pad placement, the more productive and the more economical aircraft, and how common each type is in the sampled regions;
- the first mission-level comparison of a hybrid VTOL and a multicopter sprayer, on productivity including ground time, over farms from the United States, Brazil, Colombia and Switzerland;
- a lift+cruise sprayer built on the multicopter's parts, and the finding that its wing, in the lift rotors' wake, needs drooped flaperons to lift in rotor-borne flight;
- results bounded by the best and worst admissible pads.

Over all 180 jobs the hybrid sprayed 16.8% more hectares per hour, more on 163 of them, and used 7.8% less energy per hectare; on energy it lost on small compact farms and won once the ferry per sortie exceeded about $1.6\,\mathrm{km}$.

II. Related Work

No published work compares a hybrid VTOL with a multicopter over whole agricultural spraying missions, on energy per hectare or on productivity; existing comparisons are of steady cruise power, of flight modes within a single aircraft, or qualitative. The strands below each cover part of that question.

A. Spraying UAVs and how they are operated

A recent review names the multirotor the most suitable spraying platform, ahead of fixed-wing and VTOL aircraft, for its simple operation, safety, lack of a runway and lower cost [1]; the comparison is qualitative and leaves out flight energy. Extension guidance advises keeping ferry flights short [2], and mission research optimises the route a given aircraft flies, from coverage patterns to spot spraying and spray switching [9], [10]. Plessen splits a UAV spraying path into a spray-off transit between patches and a spraying coverage phase, and notes that near-holonomic quadrotors avoid the large turning radii of fixed-wing UAVs, while "fixed-wing UAVs might be more suited for large-scale areas" [9]. Other work covers energy-constrained coverage with a payload that drains as it is applied [11]; launch sites have been optimised over real fields [12]. In all of these the aircraft type is fixed, and where base placement is optimised the fleet is multirotor.

B. Winged VTOL aircraft for agriculture

Winged VTOLs have been reviewed as candidates for precision agriculture, with a qualitative comparison against multirotors [13]; a recent review of hybrid VTOL types names agriculture among their sectors [14]. Several agricultural designs have been proposed: a tilt-rotor plant protection UAV analysed with CFD [15], a quadplane sprayer built and flown [16], and a hybrid-wing aircraft whose downwash and droplet deposition were compared with a quadrotor's [7], [17]. None reports an energy or productivity comparison with a multicopter.

The closest work is the wing design of Yáñez Juárez et al. [6]: a $100\,\mathrm{kg}$-class multirotor carrying fixed wings and no cruise propulsor, which in CFD and a scaled wind-tunnel test needed up to 55% less power than the multirotor in steady cruise at $14\,\mathrm{m/s}$. The result supports the premise of the present study, that a wing can substantially cut a rotorcraft's power in forward flight. How that saving carries over to a whole spraying job, with its hover, spraying and ferry phases, is not addressed. Their aircraft also flies forward by pitching its rotor thrust; the present study models the hybrid as lift+cruise aircraft normally fly, with the pusher providing the thrust and the wing the lift.

C. Multicopter and winged VTOL comparisons outside agriculture

Outside agriculture, like-for-like comparisons exist. Over urban air mobility missions, a multirotor is the most efficient electric VTOL in hover and a lift+cruise aircraft a compromise [18]; at $100\,\mathrm{kg}$, winged tailsitter variants of multicopters cruise at under 40% of their hover power [5]; and in flight, a lifting wing fixed to a $2\,\mathrm{kg}$ quadrotor cut its current draw by 3.5, 29.8 and 50.1% at 5, 10 and $15\,\mathrm{m/s}$ [19]. Lift+cruise aircraft have also been optimised as whole designs [20], along energy-optimal trajectories [21] and for coverage planning [22]. These studies concern long-range, point-to-point or steady flight, or simulated area coverage without payload; none has the structure of a spraying job, mostly slow, low-level coverage with a payload that drains as it is applied.

D. Simulation of aerial vehicles

GPU-parallel simulation has made it practical to fly many aircraft at once [8]. Aerial Gym, built on Isaac Gym, simulates thousands of multirotors of arbitrary rotor layout in parallel on a GPU, for learning control and navigation [23]; OmniDrones [24] and the Pegasus Simulator [25] build multirotor platforms on Isaac Sim, the first for reinforcement learning and the second for real-time simulation with PX4; NeuralPlane does the same for fixed-wing control [26]. These tools serve learning and testing control. We found none used to compare aircraft designs over whole missions, and none that simulates a winged VTOL.

III. Terms

The following terms are used throughout the paper. A job is described at three levels:

- **mission**: the whole job on one farm, every crop area sprayed once, from the first take-off to the last landing;
- **sortie**: one flight within it, from a take-off at the pad to the landing back there, on one tank and one battery;
- **pad**: the fixed point where the aircraft takes off, lands, refills and swaps its battery.

The crop of a farm is divided into **blocks**, its separate pieces of land; a block whose shape needs it is split into **cells**, each sprayed in parallel **lanes**.

Each moment of a mission belongs to one **phase**, by what the aircraft is doing:

- **take-off and landing**: the vertical climb from the pad and descent to it;
- **spraying**: flying a lane with the spray on;
- **turns**: moving from the end of one lane to the start of the next;
- **ferry**: any flight with the spray off between two points, such as pad to crop, block to block or across a gap in a lane;
- **ground time**: on the pad, refilling and swapping the battery.

Independently of the phase, each aircraft flies in one of two **lift modes**, by what carries its weight:

- **rotor-borne**: the lift rotors carry the weight, as on any multicopter; this includes hover. The multicopter is always rotor-borne, and so is the hybrid in every phase except a wing-borne ferry; its wing may still add lift.
- **wing-borne** (hybrid only): the wing carries the weight and the pusher propeller provides the thrust, with the lift rotors stopped.

A **transition** is the change between the two: forward from rotor-borne to wing-borne, and back. The hybrid flies wing-borne only on a ferry, and only when its autopilot finds it worthwhile (Section VI).

IV. Study Design

The study pairs the two aircraft mission by mission: each flies the same route over the same farm from the same pad, under the same operating rules, and the two results are compared.

A. Metrics

A mission takes as many sorties, and so refills and battery swaps, as it needs. Each mission is scored on three measures:

- **productivity**, hectares sprayed per hour of operating time, ground time included;
- **energy**, battery energy drawn per hectare ($\mathrm{W\,h/ha}$);
- **battery swaps per hectare**.

Each mission's time and energy are also split by phase, and for the hybrid by lift mode. Flight time alone is not used as a measure, as it leaves out the ground time and would favour the aircraft that flies longer on a battery whatever it does with the time.

B. Farms

The missions are flown over 90 real farms, outlined from public parcel, cadastral and field-boundary data. They are drawn from a pool of 159,487 eligible farms ($6.61\,\mathrm{Mha}$ of crop) in the United States (Iowa and Wisconsin, 45 of the 90), Brazil (18), Colombia (17) and Switzerland (10). Only the cropped parts are sprayed. Each farm is classified by its size, in six bands of crop area A from 10 to $150\,\mathrm{ha}$, and by two measures of its layout. The **spread ratio**

$$R = \frac{d_{\mathrm{far}}}{\frac{\sqrt{5}}{2}\sqrt{A}} \tag{1}$$

TABLE I
The five farm types and their share of the eligible pool (159,487 farms, $6.61\,\mathrm{Mha}$).

Farm type	Spread ratio	Block share	Farms	Crop area
Compact	< 1.15	any	90.4%	88.1%
Moderate, consolidated	1.15–1.4	≥ 0.5	4.0%	4.6%
Moderate, fragmented	1.15–1.4	< 0.5	0.7%	1.5%
Spread, consolidated	≥ 1.4	≥ 0.5	3.8%	4.3%
Spread, fragmented	≥ 1.4	< 0.5	1.0%	1.6%

divides the distance d_{far} from the best pad (Section IV-C) to the farthest crop by the same distance for a square farm of equal area with its pad mid-edge; a farm is compact below 1.15, moderate up to 1.4 and spread above. The **block share**

$$B = \sum_i \left(\frac{a_i}{A}\right)^2 \tag{2}$$

sums over the farm's crop blocks of area a_i, crop merged across gaps under $20\,\mathrm{m}$; it is the inverse of the farm's effective number of blocks. Consolidated farms, of one or two dominant blocks, have $B \geq 0.5$; fragmented farms less. Spread and block share combine into the five farm types of Table I. Each size band holds three farms of each type, chosen as medoids within their type and country, with countries represented by their share of the type's crop area. The sample therefore covers every farm type equally and is not a population sample: how common each type is comes from the pool counts alone. Farms of more than $150\,\mathrm{ha}$ are left out: one aircraft from one pad sprays about 130 to $150\,\mathrm{ha}$ in a ten-hour working day, and larger jobs need several aircraft or a moving base.

A farm here is a set of parcels the data attribute to one holding. For farms of several blocks, the parcel data cannot always tell one operation from neighbouring operations grouped by owner; every result is therefore also reported for single-block and multi-block farms separately (42 and 48 of the 90).

C. Pad placement

Each farm is flown from two pads, the same points for both aircraft, chosen from its geometry alone before any flight. A point is a viable pad if it is not on crop and all crop lies within $2\,\mathrm{km}$ of it, the T50's maximum configurable flight radius [3]:

- the **best pad** is the viable point that minimises the distance to the farthest crop;
- the **worst pad** is the viable point on the outer edge of a crop block that maximises the mean distance to the crop, the wrong edge of the field; where no edge point is viable, the viable point anywhere that maximises it.

The two pads bound real practice rather than represent it. The best pad is the most favourable fixed pad an operator could have, and favours the multicopter, which flies every ferry rotor-borne. Real pads, at a road, a gate or a farmyard, lie between the two; access to either pad is not checked. The 90 farms and two pads give 180 missions per aircraft; Fig. 2 shows those of one size band.

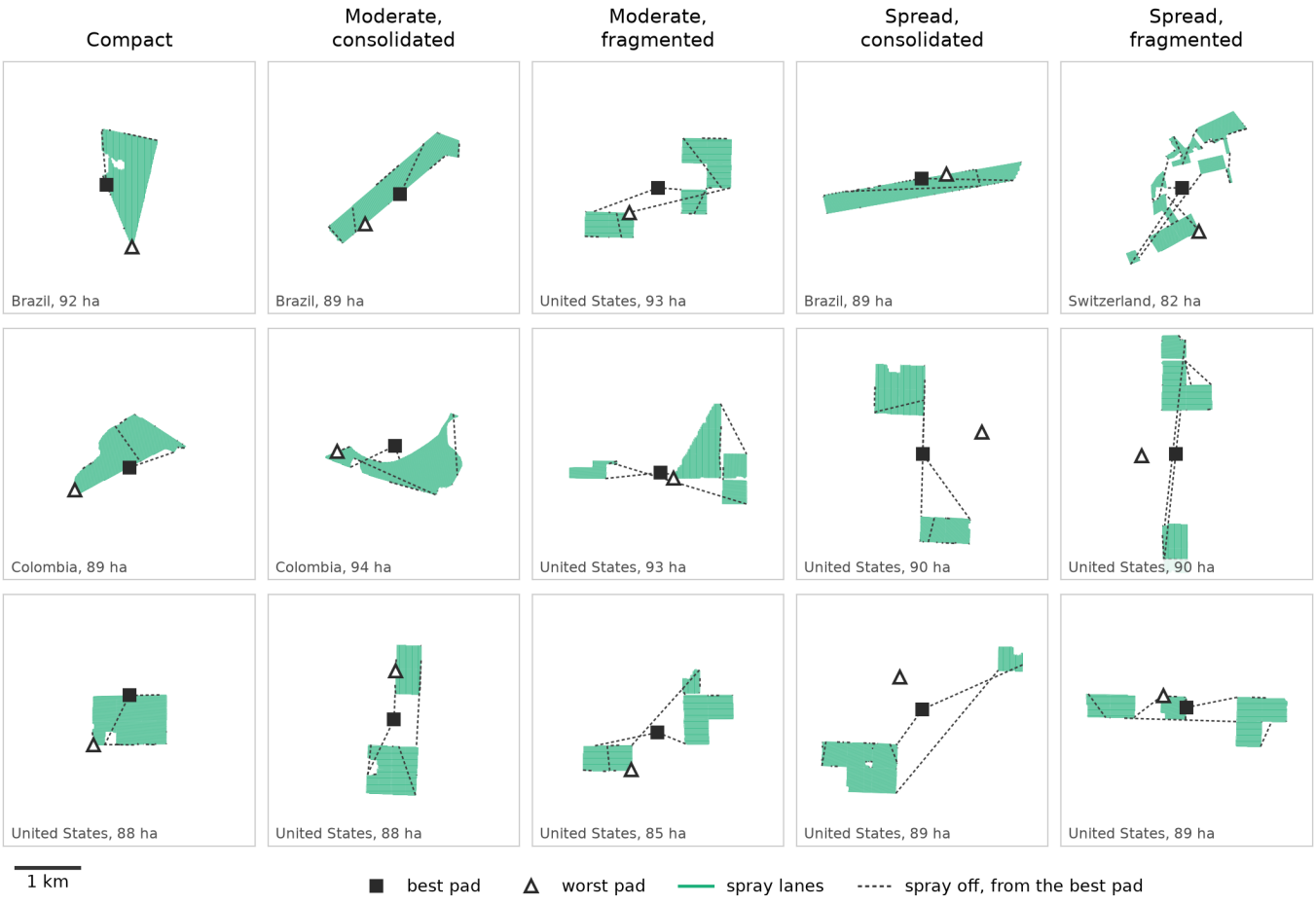

Fig. 2. The 15 farms of the 80 to 100 ha band, three of each farm type, with the route flown from the best pad (refill trips not drawn) and the position of the worst pad; all panels at the same scale.

D. Operation

Both aircraft fly under the operating rules of Table II, set to the T50's published limits where they exist. The route of each farm and pad is planned once and flown by both aircraft, the way DJI's route mode plans a field:

- parallel lanes 9 m apart, at the lane angle giving the fewest turns;
- concave blocks split into cells, so that lanes do not cross land outside the block;
- the spray on only over crop, off over gaps and in turns, as in map-based switching, with switching taken as instant [10];
- blocks flown nearest first.

Both aircraft then fly the route by Algorithm 1. Missions are not cut off: each runs until the farm is done and the aircraft is back on the pad.

The application rate, 20 L/ha (2.1 gal/acre), is at the low end of the two to five gallons per acre typical of drone spraying [27], close to the 15 L/ha of DJI's T50 productivity test [28], and within the T50's maximum flow at our speed and swath [3].

The hybrid differs only in its ferries, which it may fly wing-borne (Algorithm 2); on the lanes it flies like the multicopter, rotor-borne at the spraying speed.

Algorithm 1 A mission

```
repeat
    take off from the pad with a full tank and battery
    ferry to the first unsprayed lane
    repeat
        spray the lane, then turn to the next
    until the tank is empty or the battery holds only the return energy plus a 3% reserve
    ferry back to the pad and land
    refill and swap the battery (90 s)
until all crop is sprayed
```

E. Reporting

Results are reported mission by mission against the paired multicopter mission: by size band, farm type and pad, for single- and multi-block farms, and against the multicopter's ferry distance per sortie, on which any pad situation can be placed. How common each result is comes only from the pool counts, for the sampled regions.

V. Vehicles

Table III lists the two aircraft. Every value in the vehicle models is labelled by source: published by the manufacturer,

TABLE II
OPERATING RULES, IDENTICAL FOR BOTH AIRCRAFT.

Quantity	Value
Spraying speed	$10\,\mathrm{m/s}$ (T50 maximum)
Rotor-borne ferry speed	$10\,\mathrm{m/s}$
Lane spacing (swath)	$9\,\mathrm{m}$
Application rate	$20\,\mathrm{L/ha}$
Spraying height	$3\,\mathrm{m}$
Rotor-borne ferry height	$6\,\mathrm{m}$
Ground time per refill and swap	$90\,\mathrm{s}$
Battery reserve	3% on top of the return energy
State at each take-off	full tank, full battery
Wind	none

TABLE III
THE TWO AIRCRAFT.

	Multicopter (T50)	Hybrid
Lift rotors	8, coaxial pairs on 4 arms, 54 in	
Battery	1567 W h, 30 A h, 345 A limit	
Tank	40 L	
Mass, empty tank	52.0 kg	59.6 kg
Mass, full tank	92.0 kg	99.6 kg
Wing and tail	—	Table IV
Pusher	—	30 in, 336 N static
Wing-borne cruise speed	—	$28.5\,\mathrm{m/s}$

calibrated to a published figure, computed by CFD, derived from these, or assumed (Appendix E).

A. Multicopter

The multicopter is a model of the DJI Agras T50, built from the published specifications in its user manual [3]:

- **mass**, with and without battery;
- **rotors**: number, layout and diameter, and the wheelbase;
- **tank** volume;
- **battery**: capacity, voltage and discharge limit;
- **top speed**.

Its geometry follows DJI's published dimensions. Rotor power follows Eqs. (4)–(5). Their overall hover efficiency, 0.6195, and the battery's internal resistance, $8\,\mathrm{m\Omega}$, are calibrated to the two hover times DJI publishes: $16.5\,\mathrm{min}$ at $52\,\mathrm{kg}$ and $7\,\mathrm{min}$ at $92\,\mathrm{kg}$, which the model reproduces as 16.48 and $6.92\,\mathrm{min}$. As a check beyond the calibration, the model flies the sortie of DJI's published $21\,\mathrm{ha/h}$ operating test on 56% of its usable charge. DJI publishes no forward-flight power, so the forward-flight part of the model rests on theory; its shape was compared with published measurements of smaller multirotors (Appendix E).

B. Hybrid

The hybrid is a lift+cruise aircraft built on one rule: *every part not specific to winged flight is the T50's*. As Xiao et al. fixed a wing to an existing quadrotor to measure its effect [19], the hybrid adds a wing, a tail and a pusher to the T50's hardware.

- **Kept from the T50**: the lift rotors and motors, battery, tank, pump and nozzles, and landing gear class.
- **Added**: a wing with flaperons, a tail, a pusher propeller with its motor, and the structure that carries them.

The hybrid is $7.6\,\mathrm{kg}$ heavier, with its battery moved to keep the centre of gravity over the lift rotors.

TABLE IV
THE HYBRID'S WING AND TAIL (DESIGN D24).

Section	SD7062
Span	$3.76\,\mathrm{m}$
Chord, root / tip	$565\,\mathrm{mm}$ / $345\,\mathrm{mm}$
Area	$1.91\,\mathrm{m}^2$
Mean aerodynamic chord	$518\,\mathrm{mm}$
Aspect ratio	7.4
Incidence, root / tip	10.0° / 6.4°
Maximum lift coefficient (DATCOM)	1.50
Tail chord / span / arm	$262\,\mathrm{mm}$ / $1.86\,\mathrm{m}$ / $2.05\,\mathrm{m}$

The wing section is SD7062, chosen from seven candidates by 2D CFD (Appendix A) for its high maximum lift, which keeps the wing small, its near-best lift-to-drag ratio, and a pitching moment small enough for the tail to trim cheaply.

With the section fixed, the wing's planform (span, chord, washout and root incidence) and the tail sized to it were optimised with 3D CFD of the whole aircraft in its two main conditions: spraying rotor-borne at $10\,\mathrm{m/s}$, and trimmed wing-borne ferry flight. Each design was scored on the battery energy it would draw in one hour of flight,

$$E_\mathrm{h} = (1 - s)\, P_\mathrm{spray}\,(1\,\mathrm{h}) + e_\mathrm{ferry}\, s\, V_\mathrm{ref}\,(1\,\mathrm{h}), \qquad (3)$$

where P_spray is its battery power while spraying, e_ferry its battery energy per kilometre of wing-borne ferry at its own cruise speed, and $s = 0.064$ the share of flight time flown wing-borne in the most wing-borne operation of preliminary mission simulations (80 to $100\,\mathrm{ha}$ farms, pad up to $2\,\mathrm{km}$ away). The reference speed $V_\mathrm{ref} = 34.3\,\mathrm{m/s}$ fixes the wing-borne distance, so a slower design is not credited for covering less ground. A design counted only if it met three limits:

- **battery current** at most $345\,\mathrm{A}$, in spraying and in cruise;
- **propeller tip Mach number** at most 0.85;
- **stall margin**: a cruise speed at least 1.2 times its stall speed.

The designs leading E_h were then flown on five $10\,\mathrm{ha}$ selection missions, kept separate from the comparison, and D24, which used the least energy per hectare, was chosen (Fig. 1a, Table IV). Appendix A gives the optimisation and the comparison of the leading designs, Appendix C the mass budget.

In a first round of comparison missions, D24 used more energy per hectare than the multicopter on all 166 it flew, at every farm size and spread, against the forward-flight savings reported for winged multirotors [6], [19]. The CFD of the spraying condition showed why: the wing lies in the lift rotors' wake, and the airframe's lift falls from $94.7\,\mathrm{N}$ with the rotors off to $1.5\,\mathrm{N}$ with them running, a rotor/wing interaction known from tiltrotors [29].

This led us to a part of D24 the missions had not used: its flaperons (Fig. 3). On tiltrotors, large flap deflections were found to carry substantial lift in the rotor wake [30]. Drooped 20°, D24's flaperons restore the airframe's lift to $97.1\,\mathrm{N}$, at

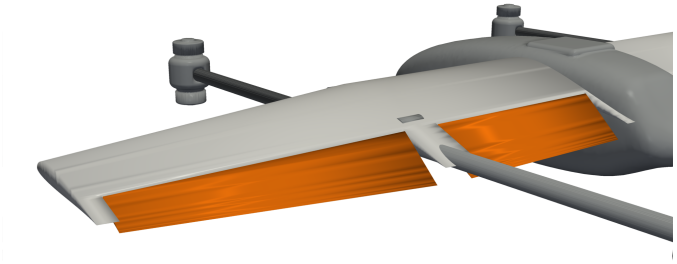

(a)

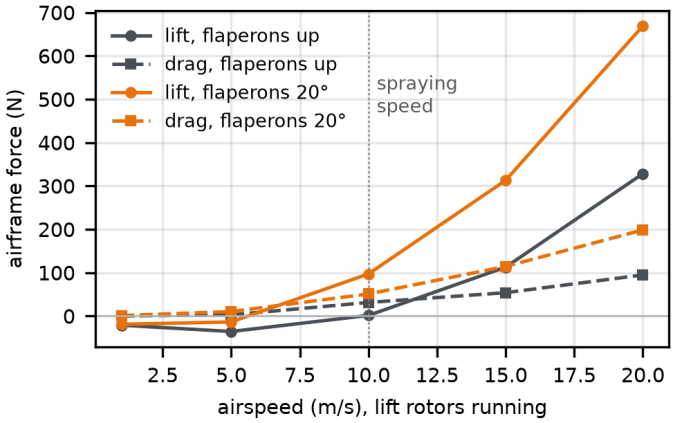

(b)

Fig. 3. D24's flaperons, two per side along the wing's trailing edge: (a) the left wing from behind, flaperons drooped 20°; (b) the airframe's lift and drag from CFD with the lift rotors running, flaperons up and at 20°.

51.0 N of drag, and cut the battery power while spraying at full tank from 9.80 to 8.70 kW, 11% less. Further CFD cases set the other flight modes, giving the schedule (droop, trailing edge down):

- **75**°: take-off, landing, hover at the pad and the rotor-borne climb;
- **20**°: spraying, turns, rotor-borne ferry, and transitions below 16 m/s;
- **up**: transitions above 16 m/s, where the droop costs more than it saves, and wing-borne flight.

C. Aerodynamics

Both aircraft's aerodynamic forces come from CFD of the full geometry, computed with OpenFOAM as steady RANS with the k–ω SST turbulence model, with the lift rotors as actuator disks at hover thrust where they run (Fig. 4). The cases each aircraft's force table needs are listed with the flight model (Tables V and VI). Because fully turbulent RANS is uncertain near stall, the hybrid's maximum lift, which sets its stall speed and so its transition speeds, is taken from the DATCOM method for its clean wing; the CFD's peak lift serves as a sensitivity case. Setup, meshes and validation are given in Appendix B.

VI. Simulation Framework

A. Flight model

The missions are flown in NVIDIA Isaac Lab [8], a GPU-accelerated simulation framework built on Isaac Sim. Each

TABLE V
CFD cases of the multicopter's force table.

Flight condition	V (m/s)	α, β	Cases
Hover, rotors on	0.5	0°, 0°	1
Forward, rotors on	5, 10	0°, 0°	2
Pitch, rotors off	10	−20, −5, 0, 20°; 0°	4
Sideways, rotors off	10	0°; 90°	1
Backwards, rotors off	10	−20, 0, 20°; 180°	3
Total			11

TABLE VI
CFD cases of the hybrid's force table; flaperons up unless stated.

Flight condition	V (m/s)	α, β	Cases
Rotor-borne			
Hover, rotors on, flaperons 75°	0.5	0°, 0°	1
Rotors on	1, 5, 10, 15, 20	0°, 0°	5
Rotors on, flaperons 20°	1, 5, 10, 15, 20	0°, 0°	5
Rotors on, flaperons 20°, pitch	10	3, 6°; 0°	2
Pitch, rotors off	10	−15, −5, 0, 5°; 0°	4
Pitch, rotors off, flaperons 20°	10	−6 to 12° by 3; 0°	7
Wing-borne			
Pitch	28.6	−6 to 18° by 3; 0°	9
Sideslip	28.6	0°; 10, 30, 90°	3
Backwards	28.6	−10, 0, 10°; 180°	3
Elevator at trim (−11.4°)	28.6	0°, 0°	1
Pusher running, stopped	28.6	0°, 0°	2
Total			42

mission is a separate environment, and many are stepped together on one GPU without interacting, as Aerial Gym does for multirotors [23]; every mission's flight log is kept and can be replayed (Fig. 1b).

Each aircraft is a rigid body stepped at 120 Hz. Its lift rotors follow their commanded thrust with a first-order lag; the airframe force is interpolated in the aircraft's CFD table (Tables V and VI) at the current airspeed V, angle of attack α and sideslip β, and for the hybrid its flaperon setting; the hybrid's pusher is limited by its motor's continuous torque.

The electrical power of each coaxial rotor pair, of thrust T and disk area A, follows momentum theory with Glauert's forward-flight inflow and a profile term,

$$v_i = \frac{T}{2\rho A\sqrt{V_t^2 + (V_a + v_i)^2}}, \tag{4}$$

$$P = \frac{1}{\eta_e}\left[\kappa\, T\,(V_a + v_i) + c_0\,\frac{T^{3/2}}{\sqrt{2\rho A}}\left(1 + 4.65\,\mu^2\right)\right], \tag{5}$$

with V_a and V_t the airspeed along and across the rotor axis, μ the advance ratio, $\kappa = 1.15$ and $\eta_e = 0.855$ for the motor

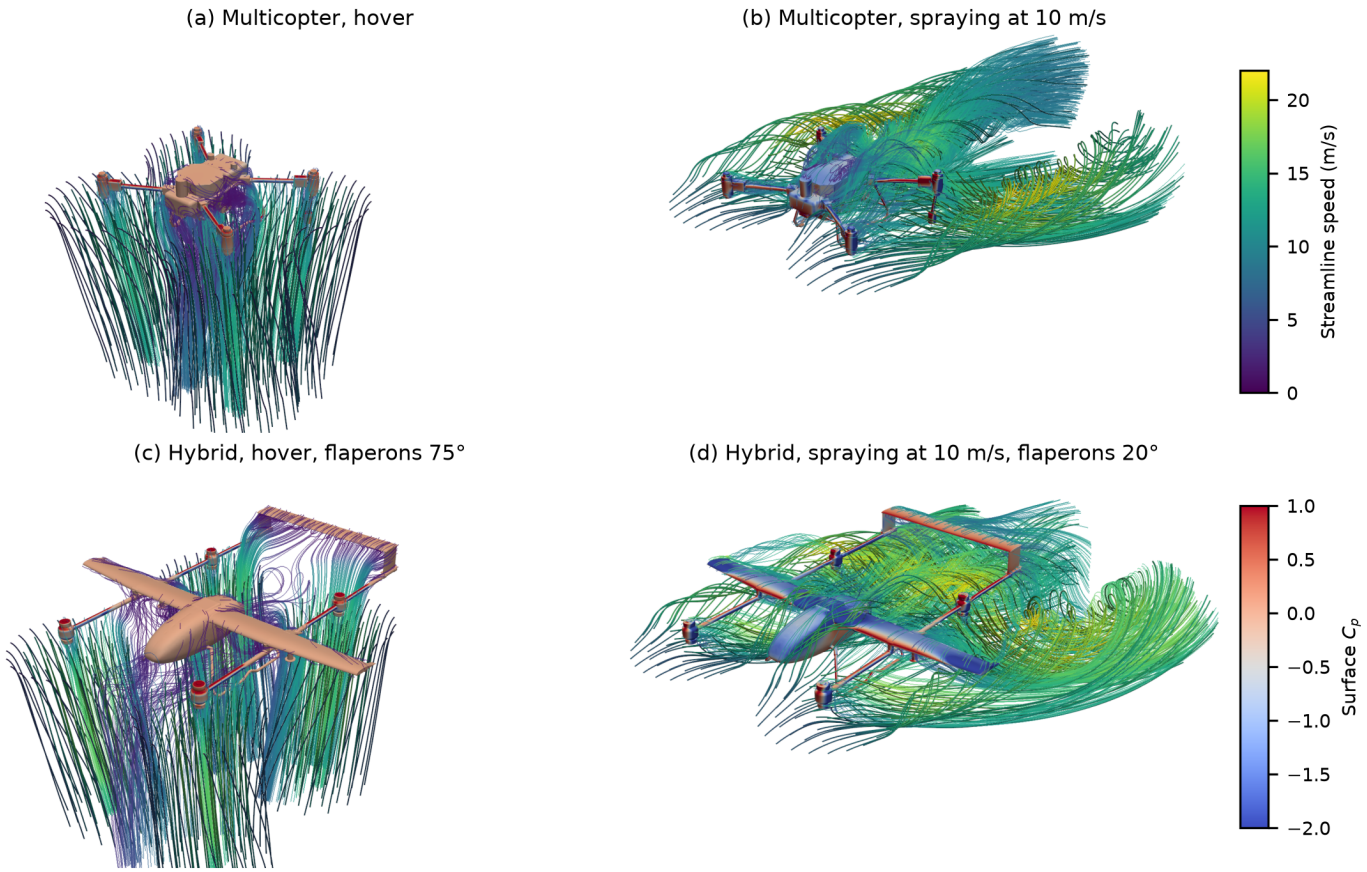

Fig. 4. CFD of the two aircraft rotor-borne, with the lift rotors as actuator disks: (a, c) hover at $0.5\,\mathrm{m/s}$; (b, d) spraying at $10\,\mathrm{m/s}$, the hybrid with its pusher thrust equal to its drag. The hybrid's flaperons are at their settings for each mode (Section V-B). Rotor thrust, split equally among the eight rotors, is $706\,\mathrm{N}$ for the multicopter ($72\,\mathrm{kg}$) and the weight of $100.4\,\mathrm{kg}$ for the hybrid. Streamlines are traced downstream from below each rotor pair (thick) and from $2\,\mathrm{cm}$ off the airframe (thin); surface C_p is referred to $10\,\mathrm{m/s}$ in all panels. Half models, mirrored.

and controller. The profile coefficient c_0 is set so that hover power matches the calibrated overall efficiency of Section V. The pack, of open-circuit voltage $E(\mathrm{SOC})$, internal resistance R and capacity Q, delivers the total power P at the current

$$I = \frac{E - \sqrt{E^2 - 4RP}}{2R}, \qquad \frac{d\,\mathrm{SOC}}{dt} = -\frac{I}{Q}, \tag{6}$$

with 85% of its charge usable; above the $345\,\mathrm{A}$ limit the thrust is cut until I meets it. While spraying, the tank drains at $q\,V\,w$, the application rate times speed times swath, so the aircraft grows lighter along every sortie.

B. Control

Both aircraft use the same cascaded position and attitude controller, with motor mixing as in ArduPilot. They differ at the lane ends:

- the **multicopter** keeps the route's heading and slides to the next lane, as in DJI's route mode;
- the **hybrid** faces the direction it flies and turns, by a flown path or a stop-and-turn, whichever is quicker, with its bank limited to $15°$ and its yaw rate to the measured $45\,°/\mathrm{s}$.

C. When the hybrid flies on its wing

Algorithm 2 gives the hybrid's ferry logic, a quadplane sequence as in ArduPilot. With m its current mass, e_w and e_r are the wing-borne and rotor-borne energy per metre from the models, and E_0 the fixed cost of a wing-borne trip (climb, transitions, settling); E_0 and the shortest wing-borne stretch $L_{\min}$, from $250\,\mathrm{m}$ with an empty tank to $490\,\mathrm{m}$ full, are measured in a sweep of single trips of different lengths and loads. $V_s = \sqrt{2mg/(\rho S C_{L,\max})}$ is the stall speed and $V_c = 28.5\,\mathrm{m/s}$ the trimmed cruise speed. Throughout, the lift rotors carry any lift the wing cannot, and the flaperons move at an assumed $60\,°/\mathrm{s}$: $20°$ below the speed V_f at which both settings cost the same power ($16\,\mathrm{m/s}$ with a full tank, $13.5\,\mathrm{m/s}$ empty), up above it.

D. Runs

Missions of similar expected length are flown together in one scene, in three steps:

- the multicopter's runs are completed and frozen, with a short reference run kept as a fingerprint;
- any later change to code the multicopter uses must reproduce the reference run bit for bit, or the multicopter runs are repeated;

Algorithm 2 A ferry stretch of length L, hybrid

if $L \geq L_{\min}(m)$ **and** $E_0(m) + e_w(m)\,L < e_r(m)\,L$ **then**
    climb rotor-borne to $10\,\mathrm{m}$
    accelerate at full pusher thrust
    at $1.2\,V_s$: wing takes over; rotors' lift share ramps to zero over $5\,\mathrm{s}$
    cruise at the energy-optimal speed in $[1.2\,V_s,\ V_c]$
    on approach: pusher off, slow on the wing to $1.1\,V_s$
    brake rotor-borne at $2\,\mathrm{m/s^2}$ to a stop at the target point
else
    fly rotor-borne at $10\,\mathrm{m/s}$ and $6\,\mathrm{m}$
end if

- the hybrid flies the same routes in the same groups and order.

A run counts only if every mission finished, with all crop sprayed and the aircraft back on its pad, within the speed and height limits and with no coverage gaps.

VII. Results

All 180 missions of both aircraft finished in Isaac Lab and passed the validity checks. Over all missions the hybrid used 7.8% less energy per hectare than the multicopter (377.0 against $408.7\,\mathrm{W\,h/ha}$) and sprayed 16.8% more hectares per hour (14.85 against 12.72), winning on energy in 111 missions and on productivity in 163.

Most sorties of both aircraft end when the $40\,\mathrm{L}$ tank is empty, so both need about one battery swap per $2\,\mathrm{ha}$. The multicopter, however, more often has to return on a low battery before its tank is empty, and the hybrid saves up to two swaps per job (Table VII): on 80 to $100\,\mathrm{ha}$ farms, one or two on 14 of the 30 jobs. It needed one swap more on a single job, a $45\,\mathrm{ha}$ fragmented spread farm from its best pad.

A. By farm type and pad

Table VII gives, for each size band, farm type and pad, what the hybrid changes per job in operating time and battery energy. On farms of 10 to $20\,\mathrm{ha}$ the differences are at most 19 minutes and about $1\,\mathrm{kW\,h}$ per job; on the largest spread farms from a poor pad the hybrid saves over two hours and $11\,\mathrm{kW\,h}$.

B. Pad placement

Moving from the best pad to the worst costs the multicopter 13% more energy per hectare and 10% of its productivity; the hybrid loses 4% on each. From the best pad the hybrid is 3.8% cheaper and 13.1% faster overall; from the worst, 11.2% cheaper and 20.3% faster.

C. Single- and multi-block farms

On the 84 missions over single-block farms, free of the doubt on whether a farm is one operation, the hybrid is 2.4% cheaper and 11.5% faster; on the 96 over multi-block farms, 11.2% cheaper and 20.7% faster. From the best pad on single-block farms the multicopter is cheaper by 2.8% and the hybrid faster by 7.0%; from the worst, the hybrid is cheaper by 6.9% and faster by 15.8%.

D. Where the difference comes from

Table VIII splits energy and time by phase. The hybrid's whole advantage is in ferry flight, where it uses 30% less energy and 39% less time, flying 43% of its ferry time wing-borne. It pays for it in the other phases: 5% more energy spraying, as it is heavier even with its flaperons drooped, and 47% more in the turns, which it flies by turning to face each new lane rather than sliding across. By size band (Fig. 5), the multicopter's ferry grows from 30% of a job's time on 10 to $20\,\mathrm{ha}$ farms to 40% on 100 to $150\,\mathrm{ha}$ farms; the hybrid saves 6 minutes of it per job on the smallest farms and 95 on the largest, while spraying and ground time are the same for both.

E. How common each case is

In the sampled regions, the farm types on which the hybrid uses less energy from either pad make up 4.2% of the eligible farms and 7.9% of their crop area; those on which it uses less only from the worst pad, a further 21.8% of farms and 39.6% of crop area. On the rest, 74.0% of farms and 52.6% of crop area, compact farms under $60\,\mathrm{ha}$ and moderate farms under $20\,\mathrm{ha}$, the multicopter is cheaper from either pad. The hybrid is faster from either pad on farm types making up 26.0% of farms and 47.4% of crop area. These shares count every multi-block farm as one operation and are therefore upper values.

VIII. Discussion

A. What it means for an operator

Table IX turns the results into a choice: a farm's size, spread ratio and block share locate its row, and the two columns give the better aircraft from the best and the worst pad. The hybrid is the clear choice on most farms from $60\,\mathrm{ha}$, and from a poorly placed pad on every farm type except compact farms under $60\,\mathrm{ha}$ and moderate farms under $20\,\mathrm{ha}$. The multicopter is the clear choice only with a good pad, on compact farms under $40\,\mathrm{ha}$ and moderate farms under $20\,\mathrm{ha}$. In between, the hybrid sprays more hectares per hour and the multicopter uses less energy per hectare, and the choice depends on which matters more to the operator.

The hybrid's clearest gain is productivity. It sprayed more hectares per hour on 163 of the 180 missions, 16.8% more overall, ground time included: at the average rates, about 149 against $127\,\mathrm{ha}$ in a ten-hour day from one pad. Its energy advantage depends on the farm, and where it holds it is felt on the pad as well as in charging: on larger farms the hybrid ends fewer sorties on a low battery and needs fewer battery swaps. The multicopter remains the cheaper aircraft per hectare on compact farms, which are nine in ten of the eligible farms, unless they are large and the pad is poor; the hybrid is cheaper wherever the aircraft must fly far between pad and crop, on spread or fragmented farms and on large ones.

B. Ferry distance as the deciding variable

Size, spread, fragmentation and pad placement all act through one quantity: the distance flown with the spray off. Against the multicopter's mean ferry distance per sortie, out and back and between blocks, the difference between the

TABLE VII
WHAT THE HYBRID CHANGES PER JOB AGAINST THE MULTICOPTER, FOR EACH FARM TYPE AND PAD: OPERATING TIME, BATTERY ENERGY DRAWN, HYBRID MINUS MULTICOPTER, THE MEAN OF THE TYPE'S THREE FARMS (NEGATIVE, THE HYBRID NEEDS LESS); BATTERY SWAPS, THE MOST THE HYBRID SAVES ON ANY OF THE THREE FARMS.

			Best pad			Worst pad		
Farm size (ha)	Spread ratio	Block share	Time (min)	Energy (kWh)	Swaps	Time (min)	Energy (kWh)	Swaps
10–20	< 1.15	any	+2	+0.7	0	0	+0.7	0
10–20	1.15–1.4	≥ 0.5	+1	+0.7	0	−3	+0.3	0
10–20	1.15–1.4	< 0.5	0	+1.0	0	−7	+0.2	0
10–20	≥ 1.4	≥ 0.5	−2	+0.4	0	−7	−0.2	0
10–20	≥ 1.4	< 0.5	−9	0.0	−1	−19	−1.1	−1
20–40	< 1.15	any	+2	+1.3	0	−7	+0.5	0
20–40	1.15–1.4	≥ 0.5	−3	+0.7	0	−17	−0.7	0
20–40	1.15–1.4	< 0.5	−6	+0.7	0	−26	−1.3	0
20–40	≥ 1.4	≥ 0.5	−9	+0.1	0	−22	−1.1	0
20–40	≥ 1.4	< 0.5	−17	−0.3	−1	−40	−2.7	−2
40–60	< 1.15	any	+1	+1.8	0	−13	+0.6	0
40–60	1.15–1.4	≥ 0.5	−12	+0.7	−1	−40	−2.1	−1
40–60	1.15–1.4	< 0.5	−17	+0.6	0	−56	−3.6	−1
40–60	≥ 1.4	≥ 0.5	−22	−0.6	−1	−33	−1.7	−1
40–60	≥ 1.4	< 0.5	−36	−1.4	−1	−46	−2.6	−1
60–80	< 1.15	any	−8	+1.8	0	−31	−0.5	0
60–80	1.15–1.4	≥ 0.5	−24	+0.1	0	−46	−2.2	0
60–80	1.15–1.4	< 0.5	−28	+0.3	−1	−55	−2.7	0
60–80	≥ 1.4	≥ 0.5	−48	−2.3	−1	−72	−4.9	−2
60–80	≥ 1.4	< 0.5	−54	−2.4	−1	−69	−3.9	−1
80–100	< 1.15	any	−19	+1.1	0	−65	−3.4	0
80–100	1.15–1.4	≥ 0.5	−34	−0.1	0	−78	−4.8	−2
80–100	1.15–1.4	< 0.5	−59	−2.6	−1	−70	−4.0	−1
80–100	≥ 1.4	≥ 0.5	−82	−5.4	−1	−103	−7.9	−1
80–100	≥ 1.4	< 0.5	−70	−3.7	−1	−87	−5.6	−1
100–150	< 1.15	any	−34	+0.6	−1	−86	−4.8	0
100–150	1.15–1.4	≥ 0.5	−60	−1.6	0	−89	−4.7	−1
100–150	1.15–1.4	< 0.5	−104	−6.6	−2	−130	−9.4	−2
100–150	≥ 1.4	≥ 0.5	−84	−4.9	−1	−91	−5.5	−1
100–150	≥ 1.4	< 0.5	−120	−8.3	−2	−148	−11.3	−2

TABLE VIII
ENERGY AND TIME PER HECTARE BY PHASE, ALL 180 MISSIONS.

	Energy (W h/ha)		Time (min/ha)	
Phase	Multicopter	Hybrid	Multicopter	Hybrid
Spraying	196.5	206.4	1.94	1.92
Turns	22.5	33.1	0.18	0.22
Ferry	180.8	127.1	1.79	1.09
Take-off and landing	8.8	10.4	0.07	0.07
Ground time	—	—	0.74	0.74

aircraft falls on one nearly linear band for all farm types and both pads (Fig. 6). Each kilometre of ferry per sortie moves energy by about 14% and productivity by about 13% in the hybrid's favour; the hybrid sprays more hectares per hour beyond about $0.8\,\mathrm{km}$ and uses less energy per hectare beyond about $1.6\,\mathrm{km}$. An operator who knows how far the aircraft flies to and from the crop on each sortie can therefore read the expected difference from the figure, whatever the farm's shape or pad.

C. Sensitivity to pad placement

On moderate farms of 20 to $80\,\mathrm{ha}$, compact farms from $60\,\mathrm{ha}$ and spread consolidated farms under $40\,\mathrm{ha}$, the multicopter uses less energy, or as little, only from the best pad, and the hybrid uses less from the worst. On these farms the multicopter's advantage depends on a near-ideal pad, which is not always reachable in practice; the hybrid, which loses about 4% from a poor pad against the multicopter's 13%, is the more robust choice there. Where the multicopter wins from both pads, on compact farms under $60\,\mathrm{ha}$ and moderate farms under $20\,\mathrm{ha}$, it is simply the better aircraft on energy.

D. Moving the multicopter's base

Ferry is where the multicopter loses: even from the best pad it takes 24% of the job time on 10 to $20\,\mathrm{ha}$ farms and 37% on 100 to $150\,\mathrm{ha}$ farms. Its operators' remedy is to bring the base to the work, moving it as the spraying progresses [2]. A move is not free:

- **equipment**: a truck, trailer, generator and tanks, $25,500 to $36,000 against $23,000 for the drone [4];
- **crew**: a pilot and a visual observer [31], at $30 per hour each [4];
- **time**: $10\,\mathrm{min}$ to tear down and $10\,\mathrm{min}$ to set up [32], plus the drive.

A move thus trades ferry time for moving time. Our missions are flown from one fixed pad and do not simulate moves, so to compare the two operations we give the multicopter the

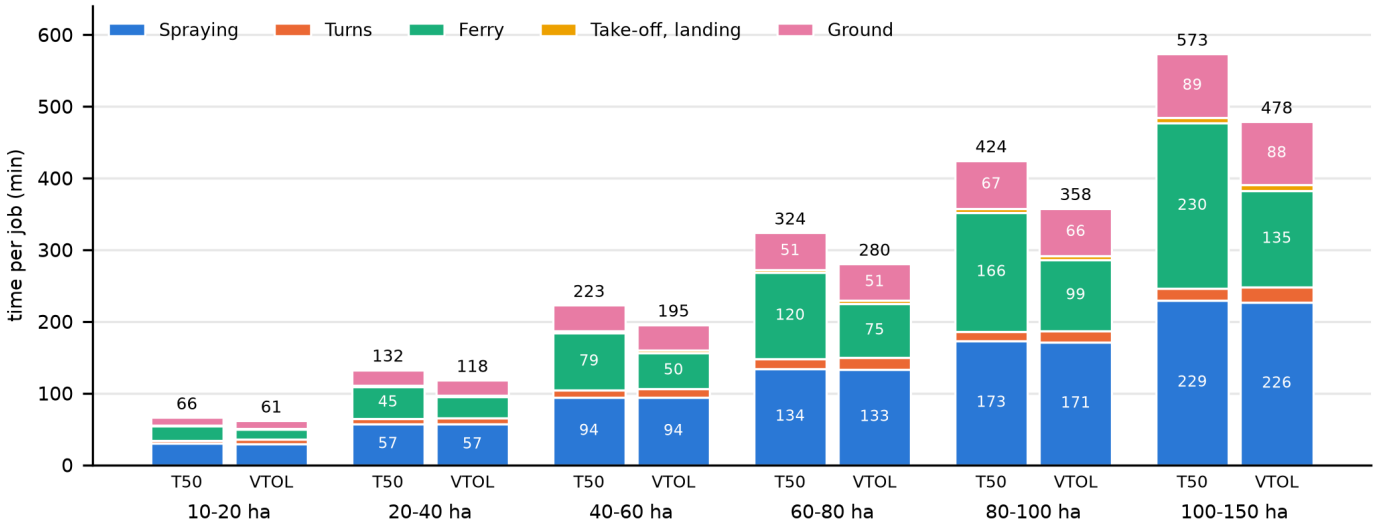

Fig. 5. Time per job by phase and size band, mean of the band's 30 jobs over both pads; totals above the bars.

TABLE IX

THE BETTER AIRCRAFT FOR EACH FARM TYPE, FROM THE BEST AND THE WORST PAD: T50, THE MULTICOPTER; VTOL, THE HYBRID. WHERE ONLY ONE MEASURE IS NAMED, THE TWO ARE WITHIN 2% ON THE OTHER.

Farm size (ha)	Spread ratio	Block share	Best pad	Worst pad
10–20	< 1.15	any	T50	T50 (energy)
10–20	1.15–1.4	≥ 0.5	T50	VTOL (speed) / T50 (energy)
10–20	1.15–1.4	< 0.5	T50 (energy)	VTOL (speed) / T50 (energy)
10–20	≥ 1.4	≥ 0.5	VTOL (speed) / T50 (energy)	VTOL
10–20	≥ 1.4	< 0.5	VTOL (speed)	VTOL
20–40	< 1.15	any	T50	VTOL (speed) / T50 (energy)
20–40	1.15–1.4	any	VTOL (speed) / T50 (energy)	VTOL
20–40	≥ 1.4	any	VTOL (speed)	VTOL
40–60	< 1.15	any	T50 (energy)	VTOL (speed) / T50 (energy)
40–60	1.15–1.4	any	VTOL (speed) / T50 (energy)	VTOL
40–60	≥ 1.4	any	VTOL	VTOL
60–80	< 1.15	any	VTOL (speed) / T50 (energy)	VTOL
60–80	1.15–1.4	any	VTOL (speed)	VTOL
60–80	≥ 1.4	any	VTOL	VTOL
80–100	< 1.15	any	VTOL (speed) / T50 (energy)	VTOL
80–100	1.15–1.4	≥ 0.5	VTOL (speed)	VTOL
80–100	1.15–1.4	< 0.5	VTOL	VTOL
80–100	≥ 1.4	any	VTOL	VTOL
100–150	< 1.15	any	VTOL (speed)	VTOL
100–150	≥ 1.15	any	VTOL	VTOL

best case: its moves remove all the ferry it flew from the best pad, and each move costs only 20 min of teardown and set-up, with no driving. Under these assumptions, and ignoring the equipment, crew and driving each move costs, the moving multicopter stays ahead of the hybrid flying from a single pad only while it moves less than about once per 20 ha (Fig. 7). On 14 of the 15 farms of 10 to 20 ha, a single move already leaves it the longer job. On 100 to 150 ha farms its margin is about six moves, which would have to bring the base beside the lanes of some 60 sorties. A single-pad hybrid needs none of this: one site, one set-up, and no truck following the work.

E. Designing a winged sprayer

A wing chosen for cruise alone would have missed the result. Mounted among the lift rotors, the wing lost almost all its lift in rotor-borne flight, the phase in which a sprayer spends most of its time, and only drooped flaperons recovered it. Even so, the hybrid spends 5% more energy than the multicopter while spraying and 47% more in the turns. The first is the cost of carrying the wing at spraying speed; the second comes from turning to face each lane, flown here under an assumed 15° bank limit. Both are the natural targets for a next design.

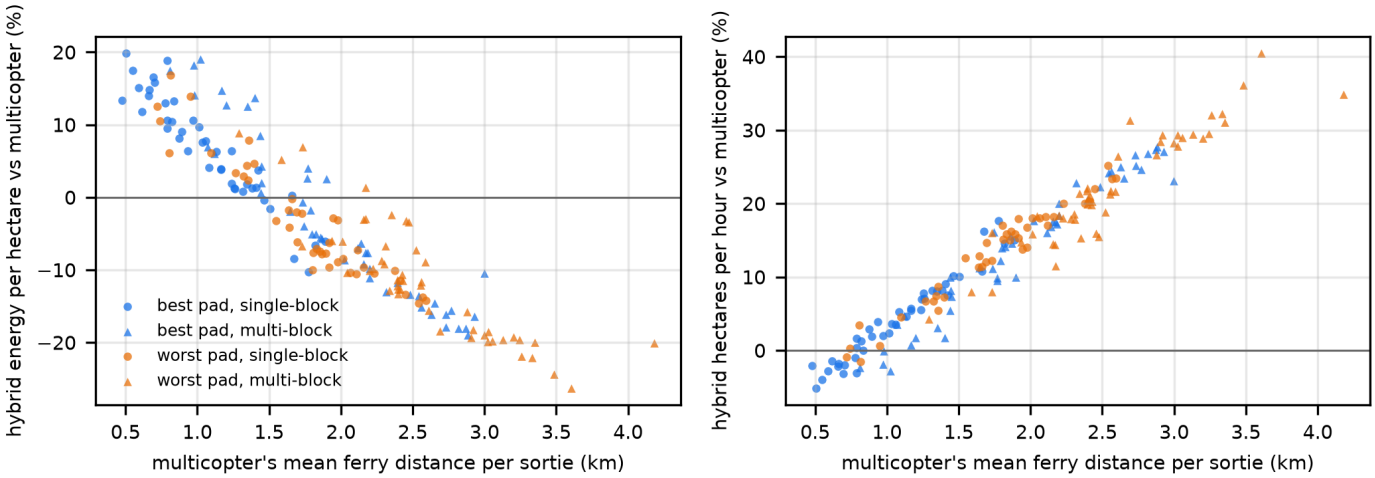

Fig. 6. Hybrid against multicopter for each of the 180 missions, against the multicopter's mean ferry distance per sortie (out and back, and between blocks).

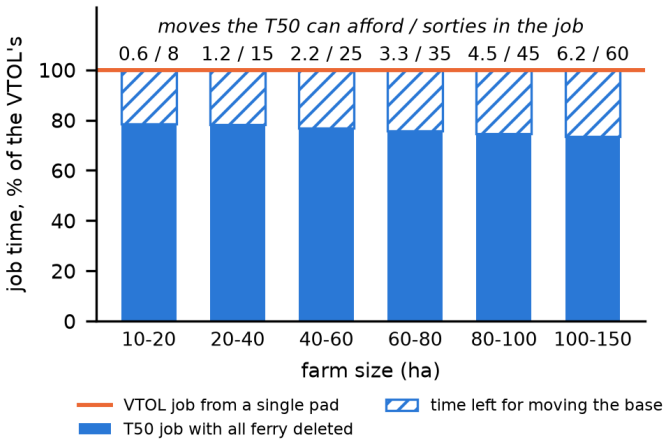

Fig. 7. The multicopter's job with all ferry deleted, against the hybrid's job from a single pad (its best), mean of each size band's 15 farms. The gap is all the time left for moving the multicopter's base; above each bar, the moves it allows at 20 min of teardown and set-up each [32], and the sorties they would have to serve.

IX. Limitations and Future Work

A. Limitations

The main limitation is that every result is simulated: neither aircraft was flown. The multicopter model is calibrated to DJI's published hover times only, and the hybrid has not been built, its masses coming from CAD and its forces from CFD. Within the simulation:

- **Models:** the multicopter's forward-flight power is checked only against smaller multirotors; the hybrid's bank limit and flaperon rate are assumed; stall is taken from DATCOM, as the CFD is steady.
- **No wind.**
- **Farms:** multi-block farms are not verified as one operation, and population shares hold for the sampled regions only.
- **Pads** are placed from geometry alone, without checking access.

B. Future work

- **Wind**, which changes every ferry and acts on the hybrid's wing.
- **Rotor-assisted ferry:** ferries too short for the wing are flown rotor-borne; sharing the weight between wing and lift rotors, as in Xiao et al. [19], could make them cheaper and faster.
- **Beyond T50 parity:** lift rotors, battery and structure chosen for a winged aircraft could cut the hybrid's 7.6 kg extra mass. In the design process (Appendix A), the designs that used the least power while spraying were ruled out by the T50 battery's current limit.
- **A built hybrid**, weighed and with its power measured, to test the model.
- **Route planning:** refining the block order and the coverage pattern, as in Plessen [9], [10], would shorten both aircraft's in-field legs; only moving the pad shortens the flight from pad to crop.
- **Wider scope:** farms over 150 ha, and pads checked for road access.

X. Conclusion

Over 180 spraying jobs on 90 real farms, simulated in Isaac Lab, a lift+cruise hybrid built from a DJI Agras T50's parts sprayed 16.8% more hectares per hour than the T50 and used 7.8% less energy per hectare. Its advantage grows with the distance flown between pad and crop: it sprays more hectares per hour beyond about 0.8 km of ferry per sortie and uses less energy per hectare beyond about 1.6 km. The multicopter remains the more economical choice on small compact farms with a good pad, which are most farms by number; the hybrid is the better choice on large, spread or fragmented farms and whenever the pad cannot be placed well. Reaching this required a wing designed for rotor-borne flight as well as cruise: in the lift rotors' wake the wing lost its lift, and drooped flaperons recovered it.

TABLE X
THE SEVEN CANDIDATE SECTIONS IN 2D CFD: MAXIMUM LIFT, AND PITCHING MOMENT AT $\alpha = 0^\circ$, AT A REYNOLDS NUMBER OF ONE MILLION; BEST LIFT-TO-DRAG RATIO AT EACH REYNOLDS NUMBER.

		$(L/D)_{\max}$ at Re (million)			
Section	$C_{L,\max}$	0.6	1.0	1.6	$C_{m,0}$
FX 63-137	1.89	86	98	107	-0.240
SD7062	**1.68**	**78**	**90**	**101**	$\mathbf{-0.094}$
NACA 4412	1.49	82	93	99	-0.114
NACA 64_2-415	1.46	79	87	95	-0.090
NACA 4415	1.45	76	86	91	-0.114
NACA 4418	1.43	68	77	83	-0.086
NACA 23015	1.32	56	63	69	$+0.011$

APPENDIX A
DESIGN OF THE HYBRID'S WING

A. Wing section

The section was chosen before the planform, by 2D CFD of seven candidates covering the usual families for a wing of this size: the NACA 4412, 4415 and 4418 (four-digit, 12 to 18% thick), the NACA 23015 (five-digit, camber far forward), the NACA 64_2-415 (laminar flow), the Wortmann FX 63-137 (high lift, strongly cambered) and the Selig–Donovan SD7062 (low Reynolds number).

Each section was run in OpenFOAM on a body-fitted C-grid as steady RANS with the k–ω SST turbulence model and the Langtry–Menter transition model (free-stream turbulence 0.07%), with the first cell scaled with Reynolds number to hold y^+ constant. The cases cover Reynolds numbers of 0.6, 1.0 and 1.6 million, the wing's mean chord over its likely speeds, at angles of attack from -2° to 18° in 2° steps: 231 cases, none of which failed. The same setup was checked on the NACA 0012 at a Reynolds number of 2×10^5 against XFOIL: lift was within 3% at 4° and 12% low at 8°, drag 11 to 16% high, and a refinement from 58,000 to 292,000 cells changed lift and drag by about 1%.

The sections were compared on three measures:

- **maximum lift**, which sets the wing area needed for a given stall speed, the area scaling with $1/C_{L,\max}$;
- **best lift-to-drag ratio**, which sets the power of wing-borne flight;
- **pitching moment** about the quarter chord, which the tail must balance in every flight condition, at a cost in tail load and trim drag.

Table X and Fig. 8 give the results. The FX 63-137 leads on maximum lift and lift-to-drag ratio, but its pitching moment, -0.240, is two and a half times SD7062's and more than twice the average of the seven (-0.104). The tail would have to balance it in every flight condition, at a cost the 2D figures do not include. Among the other six, SD7062 has the highest maximum lift at every Reynolds number (1.66 to 1.68, against at most 1.49) and a pitching moment below the seven-section average. Only the NACA 4412 has a higher lift-to-drag ratio, at 0.6 and 1.0 million; at 1.6 million SD7062 leads. The NACA 23015's near-zero pitching moment comes with the lowest maximum lift and lift-to-drag ratio of the seven. SD7062 was therefore taken as the best balance of the three measures. The 2D figures choose the section; the wing's performance on the aircraft, with its body, tail and rotors, is measured by the 3D CFD of the planform design.

B. Planform

The wing is rectangular out to the booms, then tapers to 0.61 of the root chord at the tip, twisting linearly to the tip incidence; its rear carbon rod sets a minimum chord $c_{\min}(b)$, and the tail is sized by fixed tail volumes. A design is

$$\begin{aligned} &\mathbf{x} = (b,\ c_r,\ \varepsilon,\ i_r), \\ &b \in [1.82, 4.20]\,\mathrm{m}, \quad c_r \in [c_{\min}(b), 728.6]\,\mathrm{mm}, \\ &\varepsilon \in [-4^\circ, 0^\circ], \qquad\quad i_r \in [2^\circ, 12^\circ], \end{aligned} \tag{7}$$

span, root chord, washout and root incidence. Each design is evaluated as follows:

- **CFD, spraying**: $10\,\mathrm{m/s}$, rotors as actuator disks at hover thrust, pusher equal to drag, giving P_{spray};
- **CFD, ferry**: two elevator deflections, between which the trimmed drag D and cruise speed V_c are found[1];
- **powertrain**: the pusher motor sized to the cruise thrust gives $e_{\mathrm{ferry}} = P_{\mathrm{bat}}(D, V_c)/V_c$, the battery current I and the tip Mach number M_{tip};
- **score**: E_{h} of Eq. (3), with $V_{\mathrm{ref}} = 34.32\,\mathrm{m/s}$, the start designs' median cruise speed, if $I \le 345\,\mathrm{A}$, $M_{\mathrm{tip}} \le 0.85$ and $V_c \ge 1.2\,V_s$.

The search then runs in rounds, every rule recorded before the step it governs:

1) start from 20 designs of a preliminary run, drawn from a Latin hypercube (nine within the limits);
2) fit Gaussian-process models of P_{spray}, ferry power, V_c, M_{tip}, trim and cruise lift;
3) propose two designs by expected improvement, of the spraying–ferry trade-off in round one and of E_{h} after, with the limits inside the expectation;
4) build and run both in CFD, and add them to the data;
5) stop if $\Pr\left[E_{\mathrm{h}}(\mathbf{x}) < 0.98\,E_{\mathrm{h}}^*\right] < 0.05$ for every candidate, with E_{h}^* the best measured score, or after three rounds; otherwise return to step 2.

Outcome (Fig. 9):

- the search ran its three rounds, the probability of a further 2% gain being 0.051 after the second;
- of six proposals, one broke the battery limit and five met all limits;
- the six start designs with the lowest spraying power, 10.74 to $10.89\,\mathrm{kW}$ against D24's $11.05\,\mathrm{kW}$, all broke the battery limit, drawing 519 to $817\,\mathrm{A}$ in cruise;
- the best, D24 ($b = 3.76\,\mathrm{m}$, $c_r = c_{\min} = 565\,\mathrm{mm}$, $\varepsilon = -3.6^\circ$, $i_r = 10.0^\circ$), scored $E_{\mathrm{h}} = 10.97\,\mathrm{kW\,h}$ per flight hour, with a stall margin of 1.21;
- five designs lay within 2% of it, the resolution of the trim and model errors, among them the start designs D14 ($3.54\,\mathrm{m}$, +1.6%) and D07, the best short wing ($2.54\,\mathrm{m}$, +1.95%).

[1]For half the start designs one deflection, with the elevator's effect from the other half.

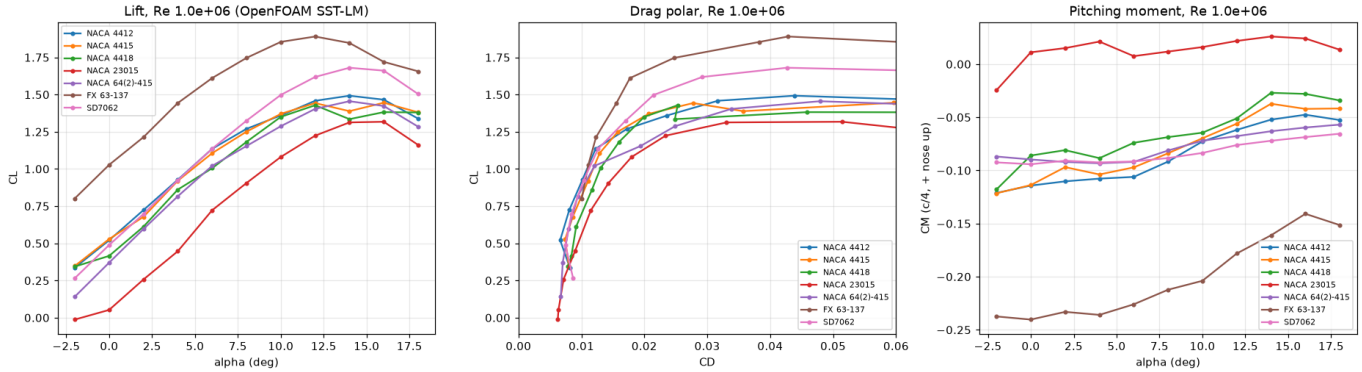

Fig. 8. The seven candidate sections in 2D CFD at a Reynolds number of one million: lift against angle of attack, drag polar, and pitching moment about the quarter chord (SST with Langtry–Menter transition).

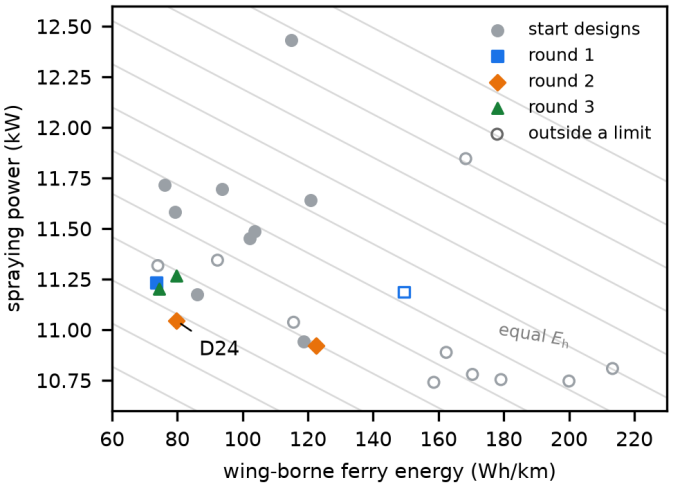

Fig. 9. The planform search: the 20 start designs and the six proposals in the plane of the two measured terms of E_{h}, with lines of equal score (lower left is better). Hollow markers break at least one limit.

D24, D14 and D07 were then flown on five $10\,\mathrm{ha}$ selection missions, one per fifth of the comparison farms' crop area by distance from the pad:

- D24 used the least energy, 491.4 against 493.3 (D14) and $507.0\,\mathrm{W\,h/ha}$ (D07), which left D07 out;
- with D14 within 2%, the two were flown again with the CFD's peak lift as the stall limit: D24 used 1.9% less (492.1 against $501.5\,\mathrm{W\,h/ha}$), won all five missions, and was taken forward.

References

[1] N. R. Gatkal, S. M. Nalawade, G. B. Bhanage, R. K. Sahni, A. A. Walunj, P. B. Kadam, and M. Ali, "Review of UAVs for efficient agrochemical spray application," *International Journal of Agricultural and Biological Engineering*, vol. 18, no. 1, pp. 1–9, 2025.

[2] J. Jackson, K. Ladino, and G. Abdulai, "General considerations and requirements for drone spraying," University of Kentucky Cooperative Extension Service, Tech. Rep. AEN-171, 2024, revised 04-2024.

[3] DJI, "AGRAS T50/T25 user manual v1.0," https://dl.djicdn.com/downloads/t50_t25/20240201/T50_T25_User_Manual_v1.0_EN.pdf, 2024.

[4] University of Missouri Extension, "Economics of drone ownership for agricultural spray applications," University of Missouri Extension, Tech. Rep. G1274, 2025. [Online]. Available: https://extension.missouri.edu/publications/g1274

[5] S. K. Rohith, A. Sridharan, and B. Govindarajan, "Hybrid powertrain systems for 100 kg multicopters and tailsitters," *Journal of Aircraft*, vol. 63, no. 2, pp. 575–591, 2026.

[6] G. A. Yáñez Juárez, A. A. Castro De La Cruz, L. Pérez-Domínguez, and A. Paz Pérez, "Aerodynamic wing design for an unmanned aerial vehicle for agricultural applications," *Drones*, vol. 10, no. 5, p. 373, 2026.

[7] J. Hao and Y. Li, "Numerical simulation analysis of droplet spraying by an agricultural hybrid wing unmanned aerial vehicle," *AIP Advances*, vol. 14, no. 11, 2024.

[8] NVIDIA, M. Mittal, P. Roth, J. Tigue, A. Richard *et al.*, "Isaac lab: A GPU-accelerated simulation framework for multi-modal robot learning," arXiv:2511.04831, 2025.

[9] M. Plessen, "Path planning for spot spraying with UAVs combining TSP and area coverages," arXiv:2408.08001, 2024.

[10] ——, "Predictive spray switching for an efficient path planning pattern for area coverage," arXiv:2504.00732, 2025.

[11] H. Fu, L. Zheng, W. Zhang, Y. Feng, L. Zhu, Y. Long, and J. Li, "Path planning for agricultural UAVs based on deep reinforcement learning and energy consumption constraints," *Agriculture*, vol. 15, no. 9, p. 943, 2025.

[12] E. Kolby, J. Noble, and M. Z. Li, "Optimizing agricultural drone operations: From launch and recovery siting to tiered routing strategies," arXiv:2606.20239, 2026.

[13] M. Zhou, Z. Zhou, L. Liu, J. Huang, and Z. Lv, "Review of vertical take-off and landing fixed-wing UAV and its application prospect in precision agriculture," *International Journal of Precision Agricultural Aviation*, vol. 1, no. 1, pp. 8–17, 2018.

[14] M. Osman, Y. Xia, M. Mahdi, and A. Ahmed, "Hybrid VTOL UAV technologies: Efficiency, customization, and sector-specific applications," *Alexandria Engineering Journal*, vol. 120, pp. 13–49, 2025.

[15] J. Lv, Z. Liu, Y. Lin, Y. Wei, and J. Li, "Design and simulation of agricultural plant protection UAV with tilt-rotor of increased lift and efficiency," *Journal of South China Agricultural University*, vol. 43, no. 4, pp. 125–132, 2022.

[16] S. John, M. I. Yousaf, N. Haroon, H. Rani, and U. Ahmed, "Design and development of a smart pesticide-spraying agricultural VTOL drone," in *Proc. 10th Multidisciplinary Research International Conference (MRIC)*, University of Wah, Pakistan, 2025. [Online]. Available: https://www.uow.edu.pk/mric/Publications/10th%20MRIC-036.pdf

[17] J. Hao and Y. Li, "Aerodynamic analysis of the hybrid wing model for an agricultural unmanned aerial vehicle," *Journal of Physics: Conference Series*, vol. 2947, no. 1, p. 012013, 2025.

[18] A. Bacchini and E. Cestino, "Electric VTOL configurations comparison," *Aerospace*, vol. 6, no. 3, p. 26, 2019.

[19] K. Xiao, Y. Meng, X. Dai, H. Zhang, and Q. Quan, "A lifting wing fixed on multirotor UAVs for long flight ranges," in *2021 International Conference on Unmanned Aircraft Systems (ICUAS)*. IEEE, 2021, pp. 1605–1610.

[20] M. L. Ruh, D. Sarojini, A. Fletcher, I. Asher, and J. T. Hwang, "Large-scale multidisciplinary design optimization of the NASA lift-plus-cruise concept using a novel aircraft design framework," arXiv:2304.14889, 2023.

[21] A. Mathur and E. Atkins, "Energy optimal traversal between hover

waypoints for lift+cruise electric powered aircraft," arXiv:2411.08661, 2024.

[22] A. Mathur and E. M. Atkins, "Multi-mode flight simulation and energy-aware coverage path planning for a lift+cruise QuadPlane," *Drones*, vol. 9, no. 4, p. 287, 2025.

[23] M. Kulkarni, W. Rehberg, and K. Alexis, "Aerial gym simulator: A framework for highly parallelized simulation of aerial robots," *IEEE Robotics and Automation Letters*, vol. 10, no. 4, pp. 4093–4100, 2025.

[24] B. Xu, F. Gao, C. Yu, R. Zhang, Y. Wu, and Y. Wang, "OmniDrones: An efficient and flexible platform for reinforcement learning in drone control," *IEEE Robotics and Automation Letters*, vol. 9, no. 3, pp. 2838–2844, 2024.

[25] M. Jacinto, J. Pinto, J. Patrikar, J. Keller, R. Cunha, S. Scherer, and A. Pascoal, "Pegasus simulator: An Isaac Sim framework for multiple aerial vehicles simulation," in *2024 International Conference on Unmanned Aircraft Systems (ICUAS)*. IEEE, 2024, pp. 917–922.

[26] C. Xue, Q. Liu, X. Ma *et al.*, "NeuralPlane: An efficiently parallelizable platform for fixed-wing aircraft control with reinforcement learning," in *Advances in Neural Information Processing Systems 37 (Datasets and Benchmarks Track)*, 2024, pp. 96 939–96 962.

[27] J. Jackson and K. Ladino, "Drone sprayer sizing for agricultural applications," University of Kentucky Cooperative Extension Service, Tech. Rep. AEN-174, 2024, issued 03-2024.

[28] DJI, "DJI Agras T50 and T25 launch announcement," https://www.dji.com/media-center/announcements/dji-agras-t50-and-t25-en, accessed Oct. 2026.

[29] F. F. Felker and J. S. Light, "Aerodynamic interactions between a rotor and wing in hover," *Journal of the American Helicopter Society*, vol. 33, no. 2, pp. 53–61, 1988.

[30] F. F. Felker, "Wing download results from a test of a 0.658-scale V-22 rotor and wing," *Journal of the American Helicopter Society*, vol. 37, no. 4, pp. 58–63, 1992.

[31] J. Jackson, K. Ladino, T. Stombaugh, and G. Abdulai, "Decision aid to determine the cost of using a drone sprayer in production agriculture," University of Kentucky Cooperative Extension Service, Tech. Rep. AEN-172, 2024, revised 04-2024.

[32] J. Deveau, "Drone tendering: Considerations before buying or building," Sprayers 101, https://sprayers101.com/drone-tender/, accessed Oct. 2026.